



JMRA

Journal of Mechanical Research and Application

ISSN: 2251-7383, eISSN: 2251-7391



Forced Vibration Analysis of Functionally Graded Rectangular Plates with Porosities under a Moving Load

Ali Akhgary¹, Ahmad Reza Khorshidvand^{2*}

1- Department of Mechanical Engineering, Science and Research Branch, Islamic Azad University, Tehran, Iran

2- Department of Mechanical Engineering, South Tehran Branch, Islamic Azad University, Tehran, Iran

(Email: Ar_Khorshidvand@azad.ac.ir)

Received: 2020-09-01

Accepted: 2020-09-04

Abstract: In this paper, vibration behaviors of functionally graded rectangular plates with porosity under a moving concentrated load are considered. Mechanical properties such as elasticity modulus and density of functionally graded (FG) plates are varied as power-law, while Poisson's ratio is kept constant and porosity as two types of evenly distribution (porosity-I) and unevenly distribution (porosity-II) is assumed. Based on first order shear deformation theory (FSDT) and by employing Hamilton's principle, the theoretical equations of motion and boundary conditions are derived. Dimensionless discrete equations have been achieved by using generalized differential quadrature method and Newmark procedure. The convergence and accuracy of the present formulation and method of the solution are demonstrated. The effect of volume fraction index, porosity volume fraction and distribution pattern on displacements of plates have been investigated. It is discovered that the volume fraction index has a significant effect on the deflection of the plates and the porosity volume fraction influences more significantly on deflection of porous FG plates in porosity-I than in porosity-II.

Keywords: Porous functionally graded plates, Moving load, First order shear deformation theory, Differential quadrature method

1. Introduction

Nowadays, studies on thermo mechanical behavior of porous functionally graded materials and the investigation of porosity effect on the response of such different structures are developing due to the wide application of them. Esmaeilzadeh M, Kadkhodayan M. [1] investigated the nonlinear dynamic behaviors of eccentrically stiffened rectangular porous bi-directional FG plates under a moving load with a constant velocity. They derived the governing of differential equations through Hamilton's principle based on the FSDT and Von Karman relations for large deflections and used dynamic relaxation method with kinetic damping (K-DR) coupled with Newmark integration technique, to solve time-varying nonlinear equations. They investigated effects of some research parameters on dynamic behaviors and showed that dynamic behaviours of the porous bi-directional FG plates improved highly with the aid of eccentric stiffeners. Shahbazzabar A,

Ranji AR. [2] extended the applications of differential quadrature element method to study the vibrational response of FG rectangular plates resting partially on elastic foundations. DinhDuc N, Quang VD, Nguyen PD, Chien TM. [3] presented an analytical approach to evaluate natural frequencies and nonlinear dynamic responses of a simply supported FG plate subjected to thermal and mechanical loading using FSDT by using Von Karman geometrical nonlinearity formulations. Hien TD, Lam NN. [4] Presented an analytical solution for the dynamic responses of FG rectangular plates supported with a viscoelastic foundation subjected to concentrated moving loads. They assumed that material properties vary through the thickness according to the power-law function and by using Hamilton's principle derived constitutive relations based on higher-order shear deformation and solved them by using state-space methods. They also discussed various structural parameters on displacement of the plate. Eftekhari SA, Jafari AA. [5] Presented a simple, efficient, precise mixed Ritz-DQ method for free and forced vibration analysis of rectangular plates.

In present study, a numerical solution for the forced vibration response of FG rectangular plate with evenly and unevenly distributed of porosities under a moving load is developed. The linear equations of motion are derived based on the FSDT by utilizing Hamilton's principle. The governing equations are solved by Newmark, and differential quadrature methods. The results are compared with previous studies and the effects of different parameters such as material graded index, porosity distribution coefficient and patterns on displacement of FG plates are investigated.

2. FUNDAMENTAL EQUATIONS OF FGM PLATES WITH POROSITIES

2.1. FGM Plates with Porosities

As shown in Figure 1(a), a functionally graded rectangular plate consisting of two components ceramic and metal is considered. The geometry of the plate and coordinate system are illustrated in Figure 1(a).

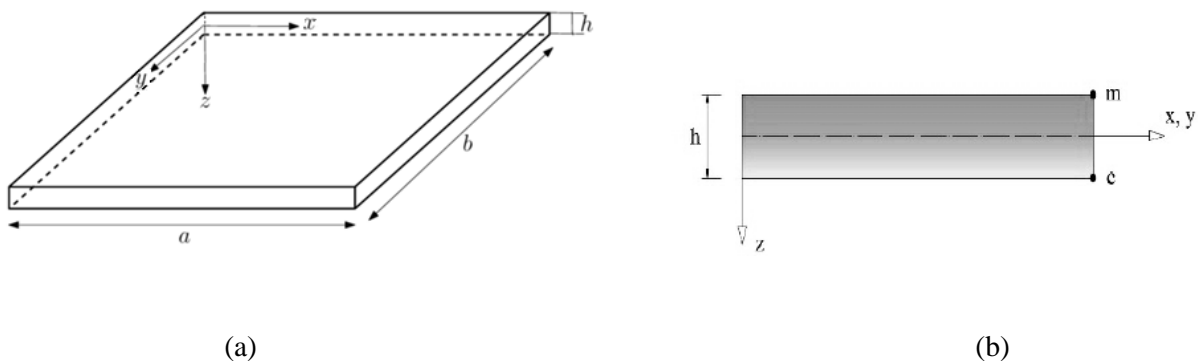
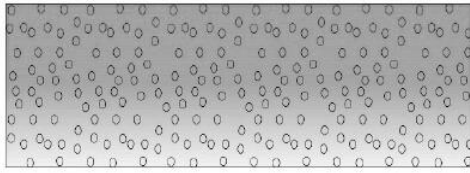


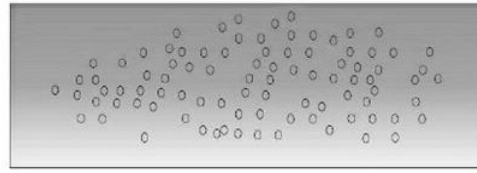
Figure 1. (a) Geometry and coordinate system of the FGM. (b) Power-law distribution of the FGM plate

For a plate made from two different constituent materials, the volume fraction is assumed changing continuously along thickness direction as it can be seen in Figure 1(b) and satisfying power-law distribution.

In this study, two porosity phases are considered including evenly distribution (porosity-I) and unevenly distribution (porosity-II) along the plate thickness direction as shown in Figure 2



(a)



(b)

Figure 2. (a) Evenly distributed porosities (porosity-I). (b) Unevenly distributed porosities (porosity-II)

Assuming porosities disperse equally in both ceramic and metal phases. The general material properties of porous FGM plate is given by [6,7]

$$P(z) = (P_c - P_m) \left(\frac{z}{h} + \frac{1}{2} \right)^n + P_m - P_{Por} \quad (1)$$

Where

$$P_{Por} = \begin{cases} \frac{\alpha}{2} (P_c + P_m) & : \text{Porosity - I} \\ \frac{\alpha}{2} (P_c + P_m) \left(1 - \frac{2|z|}{h} \right) & : \text{Porosity - II} \end{cases} \quad (2)$$

In which P_c and P_m refer to ceramic and material constituents, respectively and n is called volume fraction index ($0 \leq n \leq \infty$), also α is the porosity distribution factor. Accordingly, the young's modulus $E(z)$ and mass density $\rho(z)$ of FGM plate are stated as

$$\begin{aligned} E(z) &= (E_c - E_m) \left(\frac{z}{h} + \frac{1}{2} \right)^n + E_m - E_{Por} \\ \rho(z) &= (\rho_c - \rho_m) \left(\frac{z}{h} + \frac{1}{2} \right)^n + \rho_m - \rho_{Por} \end{aligned} \quad (3)$$

Where

$$E_{Por} = \begin{cases} \frac{\alpha}{2} (E_c + E_m) & : \text{Porosity - I} \\ \frac{\alpha}{2} (E_c + E_m) \left(1 - \frac{2|z|}{h} \right) & : \text{Porosity - II} \end{cases} \quad (5(4))$$

$$\rho_{Por} = \begin{cases} \frac{\alpha}{2} (\rho_c + \rho_m) & : \text{Porosity - I} \\ \frac{\alpha}{2} (\rho_c + \rho_m) \left(1 - \frac{2|z|}{h} \right) & : \text{Porosity - II} \end{cases} \quad (5)$$

The Poisson ratio is assumed to be constant ($\nu(z) = \nu$)

2.2. Governing Equations of Motion

The first-order shear deformation theory is used to establish governing equations based on displacement components of the plate as follows [8]

$$\begin{aligned} u(x, y, z, t) &= u_0(x, y, t) + z\theta(x, y, t) \\ v(x, y, z, t) &= v_0(x, y, t) + z\psi(x, y, t) \\ w(x, y, z, t) &= w_0(x, y, t) \end{aligned} \quad ((6))$$

Where u_0 , v_0 and w_0 are the displacement components of the middle surface in the direction of x, y and z , respectively. Moreover θ and ψ present the rotations of a transverse normal about x and y directions.

The linear strain components are computed from displacement fields in Eq. (6) and can be used in constructing the strain and kinetic energies expressions. By using the Hamilton's principle, the equations of motion are driven as follow

$$\begin{aligned} A_{11} \left[\left(\frac{\partial^2 u_0}{\partial x^2} \right) + \frac{1-\nu}{2} \left(\frac{\partial^2 u_0}{\partial y^2} \right) + \frac{1+\nu}{2} \left(\frac{\partial^2 v_0}{\partial x \partial y} \right) \right] + B_{11} \left[\left(\frac{\partial^2 \theta}{\partial x^2} \right) + \frac{1-\nu}{2} \left(\frac{\partial^2 \theta}{\partial y^2} \right) + \frac{1+\nu}{2} \left(\frac{\partial^2 \psi}{\partial x \partial y} \right) \right] - I_0 \frac{\partial^2 u_0}{\partial t^2} - I_1 \frac{\partial^2 \theta}{\partial t^2} &= 0 \\ A_{11} \left[\left(\frac{\partial^2 v_0}{\partial y^2} \right) + \frac{1-\nu}{2} \left(\frac{\partial^2 v_0}{\partial x^2} \right) + \frac{1+\nu}{2} \left(\frac{\partial^2 u_0}{\partial x \partial y} \right) \right] + B_{11} \left[\left(\frac{\partial^2 \psi}{\partial y^2} \right) + \frac{1-\nu}{2} \left(\frac{\partial^2 \psi}{\partial x^2} \right) + \frac{1+\nu}{2} \left(\frac{\partial^2 \theta}{\partial x \partial y} \right) \right] - I_0 \frac{\partial^2 v_0}{\partial t^2} - I_1 \frac{\partial^2 \psi}{\partial t^2} &= 0 \\ A_{11} \left[\kappa \frac{1-\nu}{2} \left(\frac{\partial^2 w_0}{\partial x^2} + \frac{\partial^2 w_0}{\partial y^2} \right) + \frac{\partial \theta}{\partial x} + \frac{\partial \psi}{\partial y} \right] - I_0 \frac{\partial^2 w_0}{\partial t^2} &= -P \\ A_{11} \left[-\kappa \frac{1-\nu}{2} \left(\frac{\partial w_0}{\partial x} + \theta \right) \right] + B_{11} \left[\left(\frac{\partial^2 u_0}{\partial x^2} \right) + \frac{1-\nu}{2} \left(\frac{\partial^2 u_0}{\partial y^2} \right) + \frac{1+\nu}{2} \left(\frac{\partial^2 v_0}{\partial x \partial y} \right) \right] + D_{11} \left[\left(\frac{\partial^2 \theta}{\partial x^2} \right) + \frac{1-\nu}{2} \left(\frac{\partial^2 \theta}{\partial y^2} \right) + \right. \\ \left. \frac{1+\nu}{2} \left(\frac{\partial^2 \psi}{\partial x \partial y} \right) \right] + -I_1 \frac{\partial^2 u_0}{\partial t^2} - I_2 \frac{\partial^2 \theta}{\partial t^2} &= 0 \\ A_{11} \left[-\kappa \frac{1-\nu}{2} \left(\frac{\partial w_0}{\partial y} + \psi \right) \right] + B_{11} \left[\left(\frac{\partial^2 v_0}{\partial y^2} \right) + \frac{1-\nu}{2} \left(\frac{\partial^2 v_0}{\partial x^2} \right) + \frac{1+\nu}{2} \left(\frac{\partial^2 u_0}{\partial x \partial y} \right) \right] + D_{11} \left[\left(\frac{\partial^2 \psi}{\partial y^2} \right) + \frac{1-\nu}{2} \left(\frac{\partial^2 \psi}{\partial x^2} \right) + \right. \\ \left. \frac{1+\nu}{2} \left(\frac{\partial^2 \theta}{\partial x \partial y} \right) \right] - I_1 \frac{\partial^2 v_0}{\partial t^2} - I_2 \frac{\partial^2 \psi}{\partial t^2} &= 0 \end{aligned} \quad ((7))$$

Where P is the moving load and (N_{ij}, M_{ij}, Q_{ij}) are the stress resultants and the inertias (I_i) are defined by [8]

$$(N_{xx}, N_{yy}, N_{xy}) = \int_{-h/2}^{h/2} (\sigma_{xx}, \sigma_{yy}, \sigma_{xy}) dz$$

$$(M_{xx}, M_{yy}, M_{xy}) = \int_{-h/2}^{h/2} z(\sigma_{xx}, \sigma_{yy}, \sigma_{xy}) dz$$

$$(Q_{xz}, Q_{yz}) = \kappa \int_{-h/2}^{h/2} (\sigma_{xz}, \sigma_{yz}) dz$$

$$I_i = \int_{-h/2}^{h/2} \rho(z) z^i dz, \quad i = 0, 1, 2$$

$$A_{11} = \int_{-\frac{h}{2}}^{\frac{h}{2}} \frac{E(z)}{1-\nu^2} dz; \quad B_{11} = \int_{-\frac{h}{2}}^{\frac{h}{2}} \frac{zE(z)}{1-\nu^2} dz; \quad D_{11} = \int_{-\frac{h}{2}}^{\frac{h}{2}} \frac{z^2 E(z)}{1-\nu^2} dz \quad ((8))$$

In which κ is called the shear correction factor and its most commonly used value is $\pi^2/12$.

The plate is subjected to a moving concentrated load, $P(x, y, t) = P_0 \delta(x - x_{mov}(t)) \delta(y - y_{mov}(t))$, where P_0 is the magnitude of the concentrated moving load and $(x_{mov}(t), y_{mov}(t))$ are the coordinates of the load. Symbol δ represents the Dirac delta function, integral of which is equal to unity in any neighborhood of $(x_{mov}(t), y_{mov}(t))$ and zero elsewhere [9].

2.3. Boundary Conditions

The boundary conditions used in present study is fully simply supported:

$$\begin{aligned} u_0 = v_0 = w_0 = \psi = M_{xx} = 0 & \quad \text{at } x = 0, x = a \\ u_0 = v_0 = w_0 = \theta = M_{yy} = 0 & \quad \text{at } y = 0, y = b \end{aligned} \quad ((9))$$

3. SOLUTION METHODOLOGY OF THE EQUATIONS

In this section, differential quadrature method (DQM) along with Newmark method which can solve the differential equations is proposed. In the following, the Newmark method and DQM are explained.

3.1. Differential Quadrature Method

Differential quadrature is a numerical solution method that rapidly converges to fairly accurate numerical solution of differential equations in engineering problems.

Let $\zeta(x, y)$ be a solution of a differential equation and $x_1 = 0, x_2, x_3, \dots, x_N = a$ be a set of sample points in the direction of x -axis. According to DQM, the r^{th} -order derivative of the function $\zeta(x, y)$ at point $x = x_i$ along any line $y = y_j$ parallel to the x -axis can be approximated by [10]

$$\zeta^{(r)} \Big|_{x=x_i} = \sum_{n=1}^N C_{in}^{(r)} \zeta_{nj} \quad ((10))$$

where N is the number of sample points and $C_{in}^{(r)}$ is the weighting coefficients of r^{th} -order derivative. , Quan and Chang obtained the following algebraic formulations to compute the first-order weighting coefficients [11]

$$C_{in}^{(1)} = \frac{M^{(1)}(x_i)}{(x_i - x_n)M^{(1)}(x_n)}; \quad i, n = 1, 2, \dots, N \quad \text{and} \quad i \neq n$$

$$C_{ii}^{(1)} = - \sum_{\substack{m=1 \\ i \neq m}}^N C_{im}^{(1)} ; \quad i = 1, 2, \dots, N \quad ((11))$$

where $M^{(1)}(x_i)$ is defined as

$$M^{(1)}(x_i) = \prod_{\substack{k=1 \\ k \neq i}}^N (x_i - x_k) \quad ((12))$$

3.2. The Newmark Method

In this technique, the velocity and displacement matrices at time t_{k+1} (k is the number of time steps) are approximated in terms of their values at time t_k [12]

$$\begin{aligned} \dot{x}_{k+1} &= \dot{x}_k + (1 - \alpha)h\ddot{x}_k + h\alpha\ddot{x}_{k+1} \\ x_{k+1} &= x_k + \dot{x}_k h + (0.5 - \beta)h^2\ddot{x}_k + h^2\beta\ddot{x}_{k+1} \end{aligned} \quad ((13))$$

where the coefficients α and β are parameters which determine the accuracy and stability of the numerical technique and h shows the time interval. By using Eqs. (13), the first and the second derivatives of the displacement matrix at time t_{k+1} , in terms of x_{k+1} , x_k , \dot{x}_k and \ddot{x}_k can be obtained.

3.3 The Numerical Implementation

To solve the governing equation, these equations must be in dimensionless form, then the derivatives with respect to x and y are discrete by using DQM and the derivatives with respect to t are discrete by employing Newmark method.

4. SOLVING PROCESS

After numerical implementation, governing equations Eq. (7) and boundary conditions Eq. (9) together can be rewritten in the matrix form as

$$[\mathcal{A}]\{X_{k+1}\} = [\mathcal{B}] \quad ((14))$$

where

$$\begin{aligned} [\mathcal{A}] &= \left[\frac{1}{h^2\beta} M + K \right] \\ [\mathcal{B}] &= \left[P + M \left(\frac{1}{h^2\beta} x_k + \frac{1}{h\beta} \dot{x}_k + \left(\frac{1}{2\beta} - 1 \right) \ddot{x}_k \right) \right] \end{aligned} \quad ((15))$$

In which $[M]$ is mass matrix, $[K]$ is stiffness matrix and $\{P\}$ presents the load vector based on the general form of equations of motion ($[M]\{\ddot{x}\} + [K]\{x\} = \{P\}$). Also vector $\{X\}$ includes all displacement components ($u_0, v_0, w_0, \theta, \psi$) and their derivatives with respect to x and y of entire grid points..

By using Eq. (14), the values of $\{X_{k+1}\}$ can be obtained as

$$\{X_{k+1}\} = [A]^{-1}[B] \quad ((16))$$

It should be noted the initial values for Newmark method are assumed as ($\{X_0\} = \{\dot{X}_0\} = \{\ddot{X}_0\} = 0$)

In order to do this process, a computer code is written in MATLAB environment and results are presented in following sections.

5. VALIDATION

In this section, the validity of the present study for dynamic analysis of rectangular plates under moving loads is examined. To do this, the results obtained are compared with those obtained by Eftekhari and Jafari [5]. The parameters used here are as follows

$$\frac{\rho h}{D_{11}} = 1, \quad \frac{P_0}{D_{11}} = 1, \quad a = b = 1, \quad x_{mov}(t) = vt, \quad y_{mov}(t) = 0.5$$

$$n = \alpha = 0 \quad ((17))$$

In which v is the velocity of the moving load (which is constant). It should be noted the t –axis is normalized by dividing t on T_d ($T_d = a/v$). From Figure 3, the good agreement is obtained between these two studies.

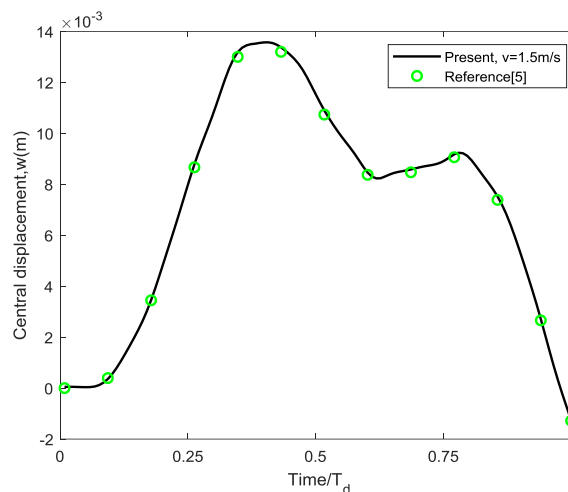


Figure 3. Comparison of numerical results for central deflection of a fully simply supported square plate subjected to a moving load

6. RESULTS AND DISCUSSION

To illustrate the present approach for deflection of porous FGM plates under a moving load, consider a fully simply supported square ceramic-metal plate ($a = b = 1, h = 0.05$) consisting of aluminum (Al) and alumina (Al_2O_3) with following properties $E_c = 380 \text{ GPa}$, $E_m = 70 \text{ GPa}$, $\rho_c = 3800 \text{ kg/m}^3$, $\rho_m = 2702 \text{ kg/m}^3$, $\nu = 0.3$, $\nu = 1 \text{ m/s}$ and $x_{mov}(t) = vt$, $y_{mov}(t) = 0.5b$ also $P_0 = 0.5 \text{ MPa}$.

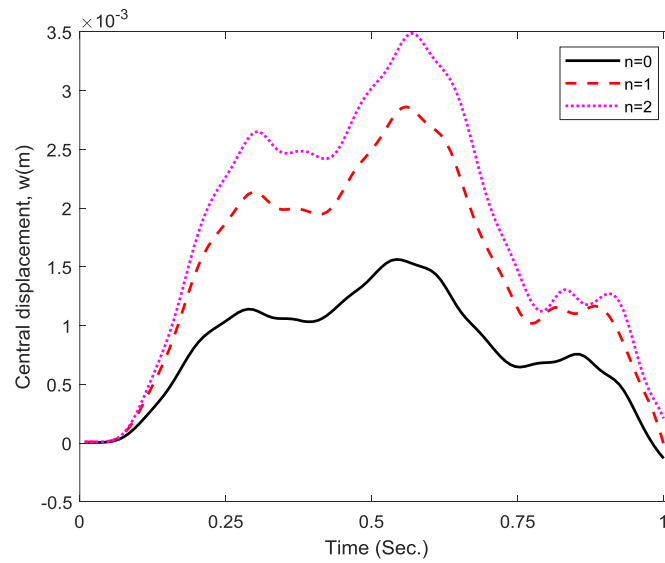


Figure 4. Effect of the volume fraction index on central deflection; ($\alpha = 0$)

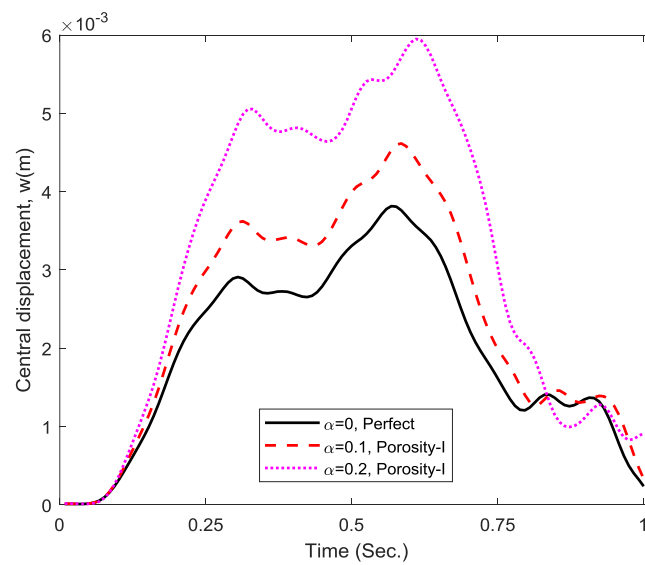


Figure 5. Effect of the porosity volume fraction on central deflection; ($n = 3$), Porosity-I

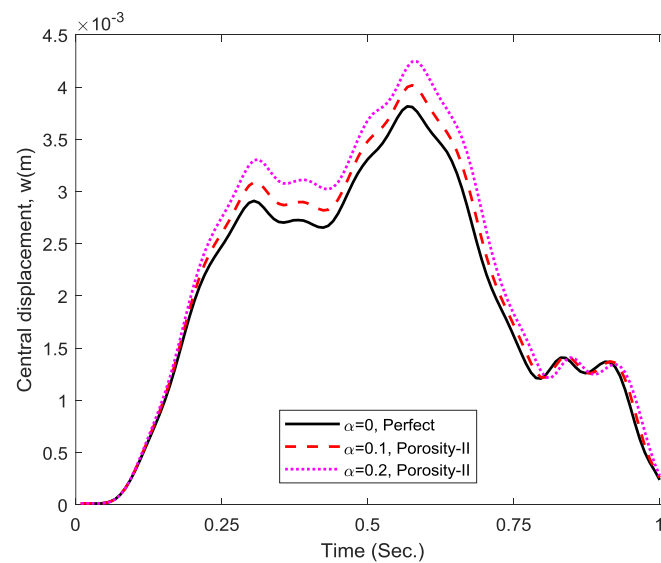


Figure 6. Effect of the porosity volume fraction on central deflection; ($n = 3$), Porosity-II

Figure (4) illustrates the effect of the volume fraction index ($n = 0, 1, 2$) on the central deflection of porous FGM plates. As can be seen, the magnitude of the deflection of FGM porous plate increase proportionally with the volume fraction index.

Figures (5) and (6) show the effect of the porosity volume fraction (α) on the central deflection of porous FGM plates. As can be observed, the higher the porosity volume fraction, the higher the magnitude of FGM plates deflection. Also the deflection of FGM plate in porosity-I phase is greater than that in porosity-II phase.

8. CONCLUSION

This paper employed first order shear deformation theory and used DQ and Newmark method to study the dynamic response of porous FG plates with two porosity phases (evenly distributed and unevenly distributed) under concentrated moving load. Comparison with other studies shows that the result of present approach are acceptable. The influences of volume fraction index and porosity volume fraction on deflection are investigated. Main finding and inferences are summarized as follow

- Volume fraction index has a significant effect on the deflection of the plates in which by increasing the volume fraction index, deflection increases.
- At the same circumstance, the maximum deflection for uneven distribution is smaller than the one for an even distribution.
- The porosity volume fraction influences more significantly on deflection of porous FG plates in porosity-I than in porosity-II.

References

- [1] Esmailzadeh M, Kadkhodayan M. Dynamic analysis of stiffened bi-directional functionally graded plates with porosities under a moving load by dynamic relaxation method with kinetic damping. Aerospace Science and Technology. 2019 Oct 1;93:105333.

- [2] Shahbazzabar A, Ranji AR. Vibration analysis of functionally graded rectangular plates partially resting on elastic supports using the first-order shear deformation theory and differential quadrature element method. *Journal of the Brazilian Society of Mechanical Sciences and Engineering*. 2019 Feb 1;41(2):102.
- [3] DinhDuc N, Quang VD, Nguyen PD, Chien TM. Nonlinear dynamic response of functionally graded porous plates on elastic foundation subjected to thermal and mechanical loads. *Journal of Applied and Computational Mechanics*. 2018 Oct 1;4(4):245-59.
- [4] Hien TD, Lam NN. Vibration of functionally graded plate resting on viscoelastic elastic foundation subjected to moving loads. *InIOP Conference Series: Earth and Environmental Science 2018 Apr (Vol. 143, No. 1, p. 012024)*. IOP Publishing.
- [5] Eftekhari SA, Jafari AA. A mixed method for free and forced vibration of rectangular plates. *Applied Mathematical Modelling*. 2012 Jun 1;36(6):2814-31.
- [6] Mechab B, Mechab I, Benaissa S, Ameri M, Serier B. Probabilistic analysis of effect of the porosities in functionally graded material nanoplate resting on Winkler–Pasternak elastic foundations. *Applied Mathematical Modelling*. 2016 Jan 15;40(2):738-49.
- [7] Shafiei N, Mousavi A, Ghadiri M. On size-dependent nonlinear vibration of porous and imperfect functionally graded tapered microbeams. *International Journal of Engineering Science*. 2016 Sep 1;106:42-56.
- [8] Reddy JN. *Mechanics of laminated composite plates and shells: theory and analysis*. CRC press; 2003 Nov 24.
- [9] Taheri MR, Ting EC. Dynamic response of plate to moving loads: structural impedance method. *Computers & structures*. 1989 Jan 1;33(6):1379-93.
- [10] Bert CW, Malik M. *Differential quadrature method in computational mechanics: a review*.
- [11] Quan JR, Chang CT. New insights in solving distributed system equations by the quadrature method—I. *Analysis. Computers & Chemical Engineering*. 1989 Jul 1;13(7):779-88.
- [12] Eslami MR. *Finite elements methods in mechanics*. Switzerland: Springer International Publishing; 2014 Jun 24.